Supplementary material for:

RADseq data reveal a lack of admixture in a mouse lemur contact zone contrary to previous microsatellite results

Table of Contents

1 Supplementary Methods

1.1 Sampling

Among the 33 allopatric additions to the Hapke et al. (2011) dataset, 13 were *griseorufus* and 20 *murinus s.l.* Ear clips from wild-caught and released mouse lemurs were collected between 2006 and 2017 (*Table S1*, *Table S2*).

The two "sympatric" sites Mangatsiaka and Tsimelahy are ~6.5 kilometers apart. Among the 49 samples from Mangatsiaka that we sequenced, Hapke et al. (2011) and Lüdemann (2018) classified 21 as *murinus* based on microsatellites as well as mtDNA, 13 as *griseorufus* based on microsatellites as well as mtDNA, 3 as *griseorufus* based on microsatellites but as *murinus* based on mtDNA (i.e. these individuals had a mitonuclear ancestry mismatch), and 14 as admixed based on the microsatellites (i.e. putative hybrids, of which 7 had a *griseorufus* mtDNA haplotype, and 7 had a *murinus* mtDNA haplotype). Among the 29 individuals from Tsimelahy, Hapke et al. (2011) classified 15 as pure *murinus*, 15 as pure *griseorufus*, and 1 as admixed based on microsatellites (this individual had a *griseorufus* mtDNA haplotype). Thus, in total, we sequenced 15 individuals for which Hapke et al. (2011) or Lüdemann (2018) had detected nuclear admixture, and an additional 3 with a mitonuclear ancestry mismatch.

Among "parapatric" sites, Hazofotsy is 14.5 kilometers from Mangatsiaka, whereas Ambatoabo is 14 kilometers from Tsimelahy (*Fig. 1* - inset). In total, we sequenced 94 samples from the contact zone area (sympatric and parapatric sites) in the Andohahela area.

1.2 Sequencing, read processing and genotyping

We prepared Restriction-site Associated DNA (RAD) sequencing libraries using 50 ng of genomic DNA from each sample following the protocol of Ali et al. (2016). Briefly, samples were digested with SbfI (New England Biolabs), followed by ligation with custom biotinylated adapters containing 8 bp barcodes unique to each sample. We pooled 48 samples in a single library, with a technical replicate for four of these samples, and sheared DNA to an average fragment size of 400 bp using a Covaris M220. RAD fragments were enriched with a streptavidin bead pull-down and prepared as a sequencing library using a NEBNext Ultra DNA Library Prep Kit (New England Biolabs). Final libraries were sequenced using paired-end 150 bp sequencing on an Illumina HiSeq 4000 at Duke University's Center for Genomic sand Computational Biology sequencing facility.

When using the Ali et al. (2016) RADseq protocol, half of the barcodes end up in the reverse (R2) reads. Therefore, raw reads in FASTQ files were first "flipped" using a custom Perl script, and

were next demultiplexed and deduplicated in `Stacks` v2.0b (Rochette et al. 2019) using the "`process_radtags`" and "`clone_filter`" commands, respectively. Reads were then quality filtered using `Trimmomatic` (Bolger et al. 2014) with the following parameters: Leading: 3, Trailing: 3, Slidingwindow: 4:15, Minlen: 60. Reads were aligned to the *M. murinus* reference genome ("Mmurinus 3.0", https://www.ncbi.nlm.nih.gov/genome/777?genome_assembly_id=308207, Larsen et al. 2017) with `BWA MEM` v0.7.15 (Li 2013). From the resulting BAM files, reads that were properly paired and had a minimum mapping quality of 30 were retained using "`samtools view`" ("-f 0x2" and "-q 30" arguments, respectively), and filtered BAM files were sorted using "`samtools sort`", all from the `SAMtools` library (v1.6, Li et al. 2009).

We performed genotype calling with `GATK` v4.0.7.0 (DePristo et al. 2011), and we filtered SNPs and individuals largely according to the "FS6" filter of O'Leary et al. (2018) (see *Supplementary Materials* for details). Unless otherwise noted, downstream analyses used sets of SNPs that resulted from this filtering procedure for all analyses except the coalescent-based modeling. The filtering procedure, which includes several consecutive rounds of removing the individuals and SNPs with the highest amounts of missing data, was performed separately for the set of all 135 sequenced individuals (including the 3 outgroup individuals; the resulting VCF was used for phylogenetic inference, admixture statistics, and served as the basic for generating full-sequence loci for coalescent-based modeling) and for the set of 94 individuals from the contact zone area (the resulting VCF was used for clustering analyses).

For the set of individuals from the contact zone area, we additionally produced two datasets using more lenient filtering procedures, to be able to examine admixture using more individuals and SNPs: (1) a dataset produced by omitting the last round of removal of SNPs and individuals based on missing data; (2) a dataset produced using the FS6 filter without the individual-filtering steps that retained two additional putative hybrids and two individuals with mitonuclear discordance.

We computed the following quality control statistics for each sample and then compared these between samples that had previously been identified as *murinus*, as *griseorufus*, or as hybrid: number of filtered FASTQ reads, depth of coverage in BAM files, mean mapping quality, percentage of reads that were mapped, percentage of reads that were properly paired, depth of coverage, and the percentage of missing data in VCF files.

1.3 Genotype filtering

We used GATK's "HaplotypeCaller" tool to produce GVCF files for each sample. GVCF files were then merged to multi-sample, single-scaffold "*GenomicsDB Workspaces*" using GATK's "GenomicsDBImport" tool (this merging step is necessary because in GATK v4 since the joint genotyping tool n longer accepts multiple GVCF files), and these *Workspaces* were then used as input for GATK's "GenotypeGVCFs" tool, which we ran using the "--use-new-qual-calculator" option.

VCF files were filtered according to recommendations from O'Leary et al. (2018), following their "FS6" filtering steps (See Table 2 in O'Leary et al. 2018). First, we selected only SNPs (i.e., discarding structural variants) using GATK's SelectVariants tool with option "-selectType SNP". Next, we annotated the VCF file with the *Allele Balance* statistic using GATK's "VariantAnnotator" tool with option "-A AlleleBalance". The FS6 filtering procedure involved removing the following data in the following order:

1. Per-sample genotypes with a depth below 5 (using "--minDP 5" in vcftools) are are set to "missing".
2. Sites with an across-sample genotype quality (*Qual*) lower than 20 (using "--minQual 20" in vcftools).
3. Sites with an across-sample mean depth lower than 15 (using "--min-meanDP 15" in vcftools).
4. Sites/samples with specified amounts of missing data. A progressive series of filtering steps for missing data was performed, alternating between filtering at the site level (wherein sites with more than the specified percentage of missing data are removed) and filtering at the sample level (wherein sites with more than the specified percentage of missing data are removed). Site-filtering was done using "--max-missing <threshold>" in vcftools, whereas sample-filtering first required the computation of per-sample statistics on missing data (using "--missing-indv" in vcftools), followed by the removal of samples exceeding the threshold using "--remove <sample_ID>" in vcftools. Specifically, these are the maximum missing data thresholds for the consecutive filtering steps (note that this procedure is the same as in O'Leary et al.'s FS6, but the following notation is slightly different):

    a) site: 50%

b) sample: 90%

c) site: 40%

d) sample: 70%

e) site: 30%

f) sample: 50%

5. Sites with more than two alleles. Note that this step is not present in O'Leary's FS6 filter.
6. Sites not passing any of the following filters based on statistics in the "INFO" field of the VCF file.

    a) Allele balance (*ABHet* < 0.2 or *ABHet* > 0.8)

    b) Mapping quality ratio of reference vs. alternative allele (*MQRankSum* < -12.5)

    c) Strandedness of reference vs. alternative allele (*FS* > 60.0)

    d) Quality-by-depth ratio (*QD* < 2.0)

    e) Absolute mapping quality (*MQ* < 40.0)

    f) Read position of reference vs. alternative allele (*ReadPosRankSum* < -8)

These sites were set to "*FILTER*" status using `GATK`'s "`VariantFiltration`" tool followed by removal using "`--remove-filtered-all`" in `vcftools`. The threshold values used here are based on GATK guidelines (https://gatkforums.broadinstitute.org/gatk/discussion/2806/howto-apply-hard-filters-to-a-call-set), except for item a, the allele balance filter, which is not present in the GATK recommendations. For this step, we largely followed the GATK guidelines because O'Leary et al. (2018) were not always explicit about thresholds and/or performed filtering with custom procedures rather than "`VariantFiltration`" parameters. Additional minor differences with O'Leary's et al. (2018) framework are that we also included filtering based on absolute mapping score (item e above) and read position (item f above), and that we removed non-properly paired reads during BAM-file processing steps rather than in the VCF.

7. Sites with a depth higher than the mean depth plus twice the standard deviation in depth. This maximum depth threshold was computed in a first step, and sites with excessive depth were next removed using "`--max-meanDP <threshold>`" in `vcftools`.

8. A final round of filtering sites and samples with excessive missing data (as in step 5, see above) were removed using:

    a) sample: 25%

    b) site: 5%

For analyses on subsets of the data, such as the 6-species and 4-species datasets used in the `G-PhoCS` analysis, we started by subsetting the *raw* VCF with the focal samples, and then applying the filters as listed above.

For the set of samples from the contact zone area, we additionally produced two datasets using more lenient filtering procedures, to be able to examine admixture using more samples and SNPs:

1. A dataset produced by omitting the last round of removal of SNPs and samples based on missing data (i.e., step 8 above). This is referred to in the supplementary figures and tables below as "***FS7***".

2. A dataset produced using the FS6 filter without the sample-level filtering steps (in steps 4 and 8). Sample selection was instead done by taking all samples that passed the regular FS6 filter, and additionally retaining two additional putative hybrids and two samples with mitonuclear discordance with reasonable depth of coverage. This is referred to in the supplementary figures and tables below as "***rescue***".

1.4 Creating full-sequence FASTA files

To produce full-sequence FASTA files from the VCF files (i.e., including invariant sites), we used the following procedure: First, we ran the `GATK` v3.8 tool "`FastaAlternateReferenceMaker`" for each sample, producing a single-sample whole-genome fasta file based on the reference genome but replacing sites that were called as non-reference alleles in the *unfiltered* VCF file. Then, the following classes of bases were masked: (1) non-reference bases that did not pass filtering (see RADseq genotyping and filtering section above); (2) sites that were classified as non-callable using `GATK` v3.8's "`CallableLoci`" tool, using a minimum depth of 3.

Next, "loci" were extracted by (1) defining loci at an individual level as stretches of at least 25 consecutive called (non-N) bases or multiple such stretches separated by at most 10 consecutive Ns; (2) intersecting these stretches across samples, requiring at least 1 bp of overlap, and trimming from both ends any bases with fewer than 80% of focal samples represented; (3) filtering the resulting loci to include only loci that: (a) had sequences for at least 90% of focal samples, (b) were at least a 100 bp long, (c) contained at most 10% missing data, and (d) were at least 10 kbp from a neighboring locus in either direction.

Deleted: and

1.5 Ancestry assignment analyses with Structure

`STRUCTURE` performs a clustering of samples into a user defined number of clusters K, based on the genotype. The result are posterior probabilities for each sample belonging to each of the K clusters. For this analysis, no prior population information was provided, using the admixture ancestry model with independent allele frequencies and lambda set to 1. As suggested by Gilbert et al. (2012), 20 runs per K were performed, with 100 000 iterations of burn-in and 100 000 iterations after that, while K was set from 1 to 5. Selecting for the optimal number of K was done by following the Evanno et al. (2005) method of the ad hoc statistic ΔK, and the Pritchard et al. (2000) method, both implemented in the web version of `Structure Harvester` version v0.6.94 (Earl and vonHoldt 2012). For every dataset, ΔK clearly indicated K = 2 as best K, whereas the Pritchard method suggests a K = 4.

1.6 F_{ST}

Weir and Cockerham weighted F_{ST} estimates for pairwise comparisons between population groupings was calculated from VCF files using `vcftools`.

1.7 Treemix

In Treemix, admixture events among populations are inferred based on a user-defined number of admixture events. We used a number of admixture events *m* ranging from 0 to 10, and 100 bootstraps. We performed likelihood-ratio tests to determine the most likely number of migration events, comparing each graph to one with one fewer migration event, and took the first non-significant comparison as the most likely number of migration events.

1.8 Demographic Modeling

Because it was not computationally feasible to run `G-PhoCS` and `BPP` for the entire dataset, we selected 3 individuals per population with high coverage and low amounts of missing data, while ensuring that mean coverage and missing data amounts were approximately equal across populations. The species tree recovered from phylogenetic analyses was fixed for parameter sampling.

Gene flow is modelled in `G-PhoCS` using one or more discrete unidirectional migration bands between a pair of extant or ancestral lineages that overlap in time. Since each migration band adds a parameter to the model, it is often not feasible to include all possible migration bands. Here, we modelled reciprocal migration bands between *gri*-C and *mur*-C and between ancestral *griseorufus* and *murinus* lineages, as we were interested in the occurrence gene flow between *griseorufus* and *murinus* in the contact zone and in more ancient gene flow between the two species. Additionally, we ran a model with no migration bands to assess how this affected divergence time and population size estimates. We ran both models 4 times with a burn-in of 70,000 MCMC iterations. a total number of 5.4 million (no migration) and 2.9 million (migration) MCMC iterations, and the following priors as specified in the config file (which has been uploaded to Dryad) for G-PhoCS: "tau-theta-alpha 1.0", "tau-theta-beta 500.0", "mig-rate-alpha 0.002", "mig-rate-beta 0.00001", and introducing migration bands into the model after 25,000 MCMC iterations (migration parameters only apply to the model with migration bands).

The multispecies-coalescent-with-introgression (MSCi) model in BPP estimates, for each introgression event, the introgression probability φ, which represents the proportion of loci inherited from one of the two parents of an introgression node. We conducted 4 replicate runs all of which assessed support for 6 introgression events during the same periods for which gene flow was modelled in `G-PhoCS`: between the extant *mur*-C and *gri*-C populations, between the *murinus* lineage ancestral to *mur*-C and *mur*-E and the co-temporal ancestral *griseorufus* lineage, and between ancestral *murinus* and *griseorufus* lineages prior to intraspecific divergence in both species. We ran the model 4 times with a burn-in of 16,000 MCMC iterations, a total number of

1.4 million MCMC iterations, and the following priors as specified in the control (config) file (which has been uploaded to Dryad): “thetaprior = 3 0.01 e”, “tauprior = 3 0.006”, and “phiprior = 1 1”.

2 Supplementary Results

2.1 QC statistics

QC statistics were overall highly similar between *murinus*, *griseorufus*, and putative hybrid samples from the contact zone area (*Fig. S1-S10*, *Table S3*). Statistics related to read mapping were slightly lower for *griseorufus* than for *murinus*, which is expected given that the reference genome is *murinus*: the percentage of mapped reads (means of 93.4% and 93.9%, respectively; *Fig. S4*), the mean mapping quality for unfiltered BAM files (means of 44.6 and 45.8, respectively; *Fig. S5*). For these statistics, putative hybrids were intermediate, which would be expected both if they were true hybrids and if they consisted of a mixture of individuals from either species. The percentage of properly paired reads differed very little between *griseorufus* (99.76%) and *murinus* (99.85%), though these distributions barely overlapped and putative hybrids separated in two clusters (*Fig. S6*).

A lower percentage of *griseorufus* samples passed the standard filtering procedure ("FS6", 60.5% vs 83.7% for *murinus*, *Table S3*) but for samples passing these filtering steps, mean depth and the percentage of missing SNPs were similar between the two species (mean depth: 39.8x for *griseorufus* and 38.2x for *murinus*; mean percentage of missing SNPs 2.25% for *griseorufus* and 2.49% for *murinus*; *Fig. S9-S10*, *Table S4*). While putative hybrids had a slightly lower depth (34.7x) and higher missingness (2.92%) in the final VCF (*Fig. S9-S10*, *Table S4*), the absolute values are no cause of concern for subsequent analyses.

2.2 Intraspecific differentiation is more pronounced within *murinus*

`G-PhoCS` estimated a divergence time of 20.3-37.3 ka ago (95% HPD) between the contact zone area population (*mur*-C) and eastern (*mur*-E) *murinus* populations, whereas the divergence time between western (*mur*-W) and the ancestral southeastern population (*mur*-C + *mur*-E) was inferred to be much older at 162-291 ka ago (*Fig. 6A,C*). The divergence time between western (*gri*-W) and contact zone area (*gri*-C) *griseorufus* was estimated to be 43.6-79.2 ka ago. Thus, in line with `NeighborNet` results, considerably more pronounced population structure was detected within *murinus*.

Striking differences in N_e between extant populations were inferred, especially in *murinus*, where those of the two southeastern populations (*mur*-E: 13-16 k, *mur*-C: 45-53k) much smaller than that of the western (*mur*-W: 194-205 k) population (*Fig. 6A,D*). Similarly, in *griseorufus*, the

western (*gri*-W: 125-140 k) population was also inferred to be much larger than the southeastern population (*gri*-C: 46-50 k).

Overall, divergence time and population size estimates were similar for G-PhoCS models that did and those that did not incorporate gene flow (*Fig. 6C,D*) and for BPP (with gene flow); above, we presented estimates from G-PhoCS models that did incorporate gene flow. The largest differences were found for the divergence time between *murinus* and *griseorufus*, which was estimated to be 605 (95% HPD: 432-782) ka ago by G-PhoCS without accounting for gene flow, 824 (601-1081) ka ago by G-PhoCS when accounting for gene flow, and 945 (679-1238) ka ago by BPP.

3 Supplementary Tables

Table S1: Sample information: contact zone area

"put_hybrid" = putative hybrid, "sp" = species, "mgri" = *Microcebus griseorufus*, "mmur" = *Microcebus murinus*, "pop" = population designation.

ID	Sample_ID	Hapke_ID	site	pop	poptype	lat	lon	sp_radseq	sp_msat	sp_mtDNA	filter_pass	put_hybrid
mgri068	886	NA	Mangatsiaka	gri-C	sympatric	-24.963083	46.555761	mgri	mgri	mmur	fail	1
mgri069	887	NA	Mangatsiaka	gri-C	sympatric	-24.963147	46.557383	mgri	mgri	mmur	rescue	1
mgri070	889	NA	Mangatsiaka	gri-C	sympatric	-24.963244	46.557797	mgri	mgri	mgri	FS7	0
mgri071	890	NA	Mangatsiaka	gri-C	sympatric	-24.962222	46.557378	mgri	mgri	mmur	rescue	1
mgri072	2019	NA	Mangatsiaka	gri-C	sympatric	-24.962831	46.557511	mgri	mgri	mgri	FS7	0
mgri073	2020	NA	Mangatsiaka	gri-C	sympatric	-24.962650	46.557983	mgri	mgri	mgri	fail	0
mgri074	2021	NA	Mangatsiaka	gri-C	sympatric	-24.962219	46.557972	mgri	mgri	mgri	fail	0
mgri075	HZ03	Hzf_Mg_Hamb032	Hazofotsy	gri-C	parapatric	-24.841575	46.528875	mgri	mgri	mgri	FS6	0
mgri076	HZ05	Hzf_Mg_Hamb034	Hazofotsy	gri-C	parapatric	-24.828919	46.547633	mgri	mgri	mgri	FS6	0
mgri077	HZ06	Hzf_Mg_Hamb035	Hazofotsy	gri-C	parapatric	-24.828011	46.549208	mgri	mgri	mgri	FS6	0
mgri078	HZ11	Hzf_Mg_Hamb040	Hazofotsy	gri-C	parapatric	-24.841658	46.529031	mgri	mgri	mgri	FS6	0
mgri079	HZ12	Hzf_Mg_Hamb041	Hazofotsy	gri-C	parapatric	-24.841658	46.529031	mgri	mgri	mgri	FS6	0
mgri080	HZ13	Hzf_Mg_Hamb042	Hazofotsy	gri-C	parapatric	-24.842269	46.529461	mgri	mgri	mgri	FS6	0
mgri081	HZ15	Hzf_Mg_Hamb104	Hazofotsy	gri-C	parapatric	-24.841350	46.528883	mgri	mgri	mgri	fail	0
mgri082	HZ16	Hzf_Mg_Hamb105	Hazofotsy	gri-C	parapatric	-24.841350	46.528883	mgri	mgri	mgri	FS6	0
mgri083	MG05	Mtk_Mg_Hamb059	Mangatsiaka	gri-C	sympatric	-24.964172	46.557636	mgri	mgri	mgri	fail	0
mgri084	MG06	Mtk_Mg_Hamb060	Mangatsiaka	gri-C	sympatric	-24.966453	46.554600	mgri	mgri	mgri	FS6	0
mgri085	MG16	Mtk_Mg_Hamb126	Mangatsiaka	gri-C	sympatric	-24.966244	46.554728	mgri	mgri	mgri	FS6	0
mgri086	MG20	Mtk_Mg_Hamb130	Mangatsiaka	gri-C	sympatric	-24.962811	46.556350	mgri	mgri	mgri	FS6	0
mgri087	MG22	Mtk_Mg_Hamb132	Mangatsiaka	gri-C	sympatric	-24.966244	46.554728	mgri	mgri	mgri	FS6	0
mgri088	MG25	Mtk_Mg_Hamb135	Mangatsiaka	gri-C	sympatric	-24.964172	46.557636	mgri	mgri	mgri	FS6	0
mgri089	MG85	NA	Mangatsiaka	gri-C	sympatric	-24.962850	46.558133	mgri	mgri	mgri	fail	0
mgri090	Micro13	Tml_Mg_MAndo13	Tsimelahy	gri-C	sympatric	-24.951069	46.617919	mgri	mgri	mgri	FS6	0
mgri091	Micro14	Tml_Mg_MAndo14	Tsimelahy	gri-C	sympatric	-24.956069	46.610750	mgri	mgri	mgri	fail	0
mgri092	Micro19	Tml_Mg_MAndo19	Tsimelahy	gri-C	sympatric	-24.955589	46.613069	mgri	mgri	mgri	fail	0
mgri093	Micro31	Tml_Mg_MAndo31	Tsimelahy	gri-C	sympatric	-24.955589	46.613069	mgri	mgri	mgri	FS6	0
mgri094	Micro44	Tml_Mg_MAndo44	Tsimelahy	gri-C	sympatric	-24.952181	46.616931	mgri	mgri	mgri	FS6	0
mgri095	Micro58	Tml_Mg_MAndo58	Tsimelahy	gri-C	sympatric	-24.956150	46.610481	mgri	mgri	mgri	FS6	0
mgri096	Micro60	Tml_Mg_MAndo60	Tsimelahy	gri-C	sympatric	-24.951100	46.617739	mgri	mgri	mgri	FS7	0
mgri097	Micro70	Tml_Mg_MAndo70	Tsimelahy	gri-C	sympatric	-24.955931	46.611169	mgri	mgri	mgri	FS6	0
mgri098	Micro81	Mtk_Mg_MAndo81	Mangatsiaka	gri-C	sympatric	-24.968836	46.557314	mgri	mgri	mgri	FS6	0
mgri099	TM41	Tml_Mg_Hamb078	Tsimelahy	gri-C	sympatric	-24.956050	46.610808	mgri	mgri	mgri	FS6	0
mgri100	TM46	Tml_Mg_Hamb082	Tsimelahy	gri-C	sympatric	-24.955550	46.612750	mgri	mgri	mgri	FS6	0

ID	Sample_ID	Hapke_ID	site	pop	poptype	lat	lon	sp_radseq	sp_msat	sp_mtDNA	filter_pass	put_hybrid
mgri101	TM49	Tml_Mg_Hamb085	Tsimelahy	gri-C	sympatric	-24.955578	46.612522	mgri	mgri	mgri	FS7	0
mgri102	TM50	Tml_Mg_Hamb086	Tsimelahy	gri-C	sympatric	-24.955822	46.613642	mgri	mgri	mgri	FS7	0
mgri103	TM51	Tml_Mg_Hamb087	Tsimelahy	gri-C	sympatric	-24.956211	46.616492	mgri	mgri	mgri	FS6	0
mgri104	TM52	Tml_Mg_Hamb088	Tsimelahy	gri-C	sympatric	-24.956325	46.615497	mgri	mgri	mgri	FS6	0
mhyb001	2006	NA	Mangatsiaka	gri-C	sympatric	-24.963147	46.557383	mgri	hybrid	mgri	rescue	1
mhyb002	2009	NA	Mangatsiaka	mur-C	sympatric	-24.962558	46.555864	mmur	hybrid	mmur	rescue	1
mhyb003	2026	NA	Mangatsiaka	gri-C	sympatric	-24.963083	46.555761	mgri	hybrid	mgri	FS6	1
mhyb004	2027	NA	Mangatsiaka	gri-C	sympatric	-24.963339	46.557489	mgri	mgri	mgri	FS6	0
mhyb005	2033	NA	Mangatsiaka	gri-C	sympatric	-24.963339	46.557489	mgri	hybrid	mgri	fail	1
mhyb006	2034	NA	Mangatsiaka	gri-C	sympatric	-24.962981	46.557908	mgri	hybrid	mgri	FS6	1
mhyb007	MG03	NA	Mangatsiaka	mur-C	sympatric	-24.962461	46.553428	mmur	hybrid	mmur	FS6	1
mhyb008	MG15	Mtk_Mm_Hamb125	Mangatsiaka	mur-C	sympatric	-24.966886	46.554289	mmur	hybrid	mmur	FS6	1
mhyb009	MG18	Mtk_Mm_Hamb128	Mangatsiaka	mur-C	sympatric	-24.960756	46.560169	mmur	hybrid	mmur	FS6	1
mhyb010	MG24	Mtk_Mm_Hamb134	Mangatsiaka	mur-C	sympatric	-24.963300	46.555264	mmur	hybrid	mmur	FS6	1
mhyb011	MG26	Mtk_Mg_Hamb136	Mangatsiaka	gri-C	sympatric	-24.962131	46.558203	mgri	hybrid	mgri	FS6	1
mhyb012	MG27	Mtk_Mm_Hamb137	Mangatsiaka	mur-C	sympatric	-24.963703	46.554400	mmur	hybrid	mmur	FS6	1
mhyb013	MG34	Mtk_Mm_Hamb144	Mangatsiaka	mur-C	sympatric	-24.962181	46.553358	mmur	hybrid	mmur	FS6	1
mhyb014	MG50	Mtk_Mm_Hamb160	Mangatsiaka	mur-C	sympatric	-24.963556	46.553606	mmur	hybrid	mmur	FS6	1
mhyb015	MG64	Mtk_Mg_Hamb167	Mangatsiaka	gri-C	sympatric	-24.962983	46.557056	mgri	hybrid	mgri	FS6	1
mhyb016	Micro33	Tml_Mg_MAndo33	Tsimelahy	gri-C	sympatric	-24.955361	46.613989	mgri	hybrid	mgri	FS6	1
mmur037	AB01	Abt_Mm_Hamb044	Ambatoabo	mur-C	parapatric	-24.819172	46.669656	mmur	mmur	mmur	FS6	0
mmur038	AB03	Abt_Mm_Hamb046	Ambatoabo	mur-C	parapatric	-24.819172	46.669656	mmur	mmur	mmur	FS6	0
mmur039	AB04	Abt_Mm_Hamb047	Ambatoabo	mur-C	parapatric	-24.818292	46.671294	mmur	mmur	mmur	FS6	0
mmur040	AB06	Abt_Mm_Hamb049	Ambatoabo	mur-C	parapatric	-24.818869	46.664431	mmur	mmur	mmur	FS6	0
mmur041	AB12	Abt_Mm_Hamb095	Ambatoabo	mur-C	parapatric	-24.819028	46.670106	mmur	mmur	mmur	FS6	0
mmur042	AB15	Abt_Mm_Hamb098	Ambatoabo	mur-C	parapatric	-24.818292	46.671294	mmur	mmur	mmur	FS6	0
mmur043	AB16	Abt_Mm_Hamb099	Ambatoabo	mur-C	parapatric	-24.817528	46.672233	mmur	mmur	mmur	FS6	0
mmur044	AB18	Abt_Mm_Hamb101	Ambatoabo	mur-C	parapatric	-24.817575	46.672714	mmur	mmur	mmur	FS6	0
mmur045	MG17	Mtk_Mm_Hamb127	Mangatsiaka	mur-C	sympatric	-24.962792	46.558772	mmur	mmur	mmur	FS6	0
mmur046	MG19	Mtk_Mm_Hamb129	Mangatsiaka	mur-C	sympatric	-24.963703	46.554400	mmur	mmur	mmur	FS6	0
mmur047	MG23	Mtk_Mm_Hamb133	Mangatsiaka	mur-C	sympatric	-24.961067	46.559056	mmur	mmur	mmur	FS6	0
mmur048	MG28	Mtk_Mm_Hamb138	Mangatsiaka	mur-C	sympatric	-24.962811	46.556350	mmur	mmur	mmur	FS6	0
mmur049	MG42	Mtk_Mm_Hamb152	Mangatsiaka	mur-C	sympatric	-24.962181	46.553358	mmur	mmur	mmur	FS6	0
mmur050	MG49	Mtk_Mm_Hamb159	Mangatsiaka	mur-C	sympatric	-24.964047	46.553792	mmur	mmur	mmur	FS6	0
mmur051	MG58	Mtk_Mm_Hamb161	Mangatsiaka	mur-C	sympatric	-24.963556	46.553606	mmur	mmur	mmur	FS6	0
mmur052	MG65	Mtk_Mm_Hamb168	Mangatsiaka	mur-C	sympatric	-24.961622	46.556336	mmur	mmur	mmur	FS6	0

ID	Sample_ID	Hapke_ID	site	pop	poptype	lat	lon	sp_radseq	sp_msat	sp_mtDNA	filter_pass	put_hybrid
mmur053	MG66	Mtk_Mm_Hamb169	Mangatsiaka	mur-C	sympatric	-24.962247	46.556506	mmur	mmur	mmur	FS6	0
mmur054	MG67	Mtk_Mm_Hamb170	Mangatsiaka	mur-C	sympatric	-24.963133	46.558022	mmur	mmur	mmur	fail	0
mmur055	MG68	Mtk_Mm_Hamb171	Mangatsiaka	mur-C	sympatric	-24.962797	46.558875	mmur	mmur	mmur	FS6	0
mmur056	MG73	Mtk_Mm_Hamb073	Mangatsiaka	mur-C	sympatric	-24.962444	46.555161	mmur	mmur	mmur	FS6	0
mmur057	MG75	Mtk_Mm_Hamb075	Mangatsiaka	mur-C	sympatric	-24.962803	46.553764	mmur	mmur	mmur	FS6	0
mmur058	MG79	NA	Mangatsiaka	mur-C	sympatric	-24.964111	46.555672	mmur	mmur	mmur	FS6	0
mmur059	MG83	NA	Mangatsiaka	mur-C	sympatric	-24.963333	46.554697	mmur	mmur	mmur	FS7	0
mmur060	MG84	NA	Mangatsiaka	mur-C	sympatric	-24.963978	46.554981	mmur	mmur	mmur	FS7	0
mmur061	MG88	NA	Mangatsiaka	mur-C	sympatric	-24.962975	46.553869	mmur	mmur	mmur	FS6	0
mmur062	MG92	NA	Mangatsiaka	mur-C	sympatric	-24.962753	46.556922	mmur	mmur	mmur	fail	0
mmur063	Micro04	Tml_Mm_MAndo04	Tsimelahy	mur-C	sympatric	-24.956250	46.617800	mmur	mmur	mmur	FS6	0
mmur064	Micro06	Tml_Mm_MAndo06	Tsimelahy	mur-C	sympatric	-24.954511	46.620689	mmur	mmur	mmur	FS6	0
mmur065	Micro12	Tml_Mm_MAndo12	Tsimelahy	mur-C	sympatric	-24.958350	46.616369	mmur	mmur	mmur	FS6	0
mmur066	Micro24	Tml_Mm_MAndo24	Tsimelahy	mur-C	sympatric	-24.954161	46.619189	mmur	mmur	mmur	FS6	0
mmur067	Micro25	Tml_Mm_MAndo25	Tsimelahy	mur-C	sympatric	-24.948131	46.621661	mmur	mmur	mmur	FS6	0
mmur068	Micro27	Tml_Mm_MAndo27	Tsimelahy	mur-C	sympatric	-24.947961	46.621219	mmur	mmur	mmur	FS6	0
mmur069	Micro38	Tml_Mm_MAndo38	Tsimelahy	mur-C	sympatric	-24.958350	46.616369	mmur	mmur	mmur	FS6	0
mmur070	Micro49	Tml_Mm_MAndo49	Tsimelahy	mur-C	sympatric	-24.954250	46.619300	mmur	mmur	mmur	FS6	0
mmur071	Micro88	Mtk_Mm_MAndo88	Mangatsiaka	mur-C	sympatric	-24.966683	46.554583	mmur	mmur	mmur	FS6	0
mmur072	TM42	Tml_Mm_Hamb079	Tsimelahy	mur-C	sympatric	-24.948039	46.621075	mmur	mmur	mmur	FS6	0
mmur073	TM43	Tml_Mm_Hamb080	Tsimelahy	mur-C	sympatric	-24.957525	46.617106	mmur	mmur	mmur	FS6	0
mmur074	TM44	Tml_Mm_Hamb081	Tsimelahy	mur-C	sympatric	-24.954903	46.619461	mmur	mmur	mmur	fail	0
mmur075	TM47	Tml_Mm_Hamb083	Tsimelahy	mur-C	sympatric	-24.947964	46.621269	mmur	mmur	mmur	FS7	0
mmur076	TM48	Tml_Mm_Hamb084	Tsimelahy	mur-C	sympatric	-24.948575	46.620556	mmur	mmur	mmur	FS6	0
mmur077	TM53	Tml_Mm_Hamb089	Tsimelahy	mur-C	sympatric	-24.956372	46.617286	mmur	mmur	mmur	FS7	0

Table S2: Sample information: allopatric populations and outgroups
All these samples passed the FS6 VCF filter.

"pop" = population designation.

ID	Sample_ID	species	site	pop
mgan007	00-016A-8577	*ganzhorni*	Mandena	mur-E
mgan008	00-016A-875E	*ganzhorni*	Mandena	mur-E
mgan010	00-016A-8A1D	*ganzhorni*	Mandena	mur-E
mgan011	00-016A-8EBC	*ganzhorni*	Mandena	mur-E
mgan014	00072854DC	*ganzhorni*	Mandena	mur-E
mgan016	0007289B19	*ganzhorni*	Mandena	mur-E
mgan017	00074C3B6F	*ganzhorni*	Mandena	mur-E
mgan018	00074C3F7D	*ganzhorni*	Mandena	mur-E
mgan019	00074C439B	*ganzhorni*	Mandena	mur-E
mgan021	00074C54EC	*ganzhorni*	Mandena	mur-E
mgan022	00074CHC59	*ganzhorni*	Mandena	mur-E
mgri005	JMR008	*griseorufus*	Antabore	gri-W
mgri006	JMR009	*griseorufus*	Antabore	gri-W
mgri007	JMR010	*griseorufus*	Antabore	gri-W
mgri008	JMR011	*griseorufus*	Antabore	gri-W
mgri037	JMR007	*griseorufus*	Tongaenoro	gri-W
mgri040	000611B575	*griseorufus*	Tsimanampetsotsa	gri-W
mgri041	000611C0E8	*griseorufus*	Tsimanampetsotsa	gri-W
mgri043	00063932CD	*griseorufus*	Tsimanampetsotsa	gri-W
mgri044	00063935DE	*griseorufus*	Tsimanampetsotsa	gri-W
mgri045	00063983C7	*griseorufus*	Tsimanampetsotsa	gri-W
mgri046	00063999A9	*griseorufus*	Tsimanampetsotsa	gri-W
mgri047	000639B1E7	*griseorufus*	Tsimanampetsotsa	gri-W
mgri050	JMR025	*griseorufus*	Vombositse	gri-W
mgri051	JMR026	*griseorufus*	Vombositse	gri-W
mmur001	RMR44	*murinus*	Andranomena	mur-W
mmur002	RMR45	*murinus*	Andranomena	mur-W
mmur004	RMR47	*murinus*	Andranomena	mur-W
mmur006	RMR49	*murinus*	Andranomena	mur-W
mmur009	Joerg33	*murinus*	Kirindy	mur-W
mmur012	RMR27	*murinus*	Manamby	mur-W
mmur013	RMR28	*murinus*	Manamby	mur-W
mmur014	RMR29	*murinus*	Manamby	mur-W
mruf003	RMR147	*rufus*	Andrambovato	NA
mruf007	E250M100	*rufus*	Ranomafana	NA
mruf008	E250M91	*rufus*	Ranomafana	NA

Table S3: QC statistics for FASTQ, BAM, and VCF files by *microsatellite* assignment group.

statistic	*griseorufus*	hybrid	*murinus*
FASTQ: read length - mean	135.5	135.6	135.6
FASTQ: read length - median	135.6	135.6	135.6
FASTQ: read quality - mean	38.24	38.24	38.24
FASTQ: read quality - median	38.25	38.25	38.24
FASTQ: raw reads - mean	8,021,390	6,483,790	6,459,171
FASTQ: raw reads - median	7,255,766	5,966,376	6,026,840
FASTQ: dedupped reads - mean	4,133,115	3,325,910	3,279,254
FASTQ: dedupped reads - median	3,668,470	3,044,472	3,077,260
FASTQ: trimmed reads - mean	3,191,330	2,580,940	2,545,889
FASTQ: trimmed reads - median	2,902,724	2,377,917	2,379,176
BAM: mapped reads - mean	2,978,376	2,410,410	2,385,964
BAM: mapped reads - median	2,689,533	2,230,030	2,242,135
BAM: mapping % - mean	93.4 %	93.53 %	93.87 %
BAM: mapping % - median	93.38 %	93.43 %	93.79 %
BAM: properly paired % - mean	99.76 %	99.82 %	99.85 %
BAM: properly paired % - median	99.76 %	99.84 %	99.85 %
BAM: mapping quality - filtered - mean	59.22	59.2	59.21
BAM: mapping quality - filtered - median	59.22	59.18	59.2
BAM: mapping quality - unfiltered - mean	44.59	45.22	45.77
BAM: mapping quality - unfiltered - median	44.61	45.19	45.77
BAM: depth of coverage - mean	25.85	23.38	24.35
BAM: depth of coverage- median	24.9	22.41	23.61
VCF (FS6): depth of coverage - mean	39.77	34.74	38.2
VCF (FS6): depth of coverage - median	38.56	31.96	35.59
VCF (FS6): % missing SNPs - mean	2.247 %	2.917 %	2.487 %
VCF (FS6): % missing SNPs - median	1.574 %	2.549 %	1.894 %

Table S4: Filter-passing status by microsatellite assignment group.

microsatellite assignment	**standard ("FS6")**	**last filtering step omitted ("FS7")**	**FS6 + "rescue"**	**failed**	***sum***
griseorufus	23	5 (28 total)	2 (25 total)	8	38
hybrid	12	0 (12 total)	4 (18 total)	1	15
murinus	36	4 (40 total)	0 (36 total)	3	43
sum	71	9	4	12	96

Table S5: F_{ST}

A: For contact zone dataset (FS6 filter).
"sym"=sympatric, "para"=parapatric

pop 1	**pop 2**	**F_{ST}**
griseorufus – sym (n=21)	*murinus* – sym (n=33)	0.398
griseorufus – para (n=7)	*murinus* – para (n=8)	0.419
gri-C (sym+ para) (n=28)	*mur*-C (sym+ para) (n=41)	0.399

B: For dataset with contact zone and allopatric populations (FS6 filter)

	***gri*-W**	***mur*-C**	***mur*-E**	***mur*-W**
***gri*-C** (n=19)	0.060	0.461	0.504	0.436
***gri*-W** (n=14)		0.437	0.479	0.403
***mur*-C** (n=24)			0.108	0.167
***mur*-E** (n=11)				0.243
***mur*-W** (n=8)				

4 Supplementary Figures

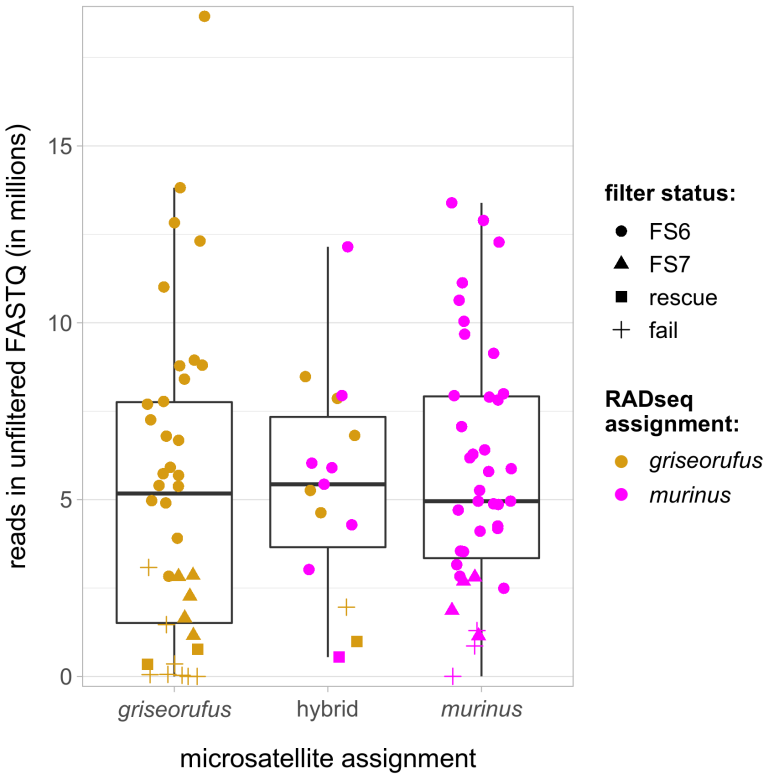

Fig. S1: Number of reads in unfiltered FASTQ files.
Comparison across microsatellite species assignments (x-axis), RADseq species assignments (color of jittered points), and filter status (shape of jittered points).

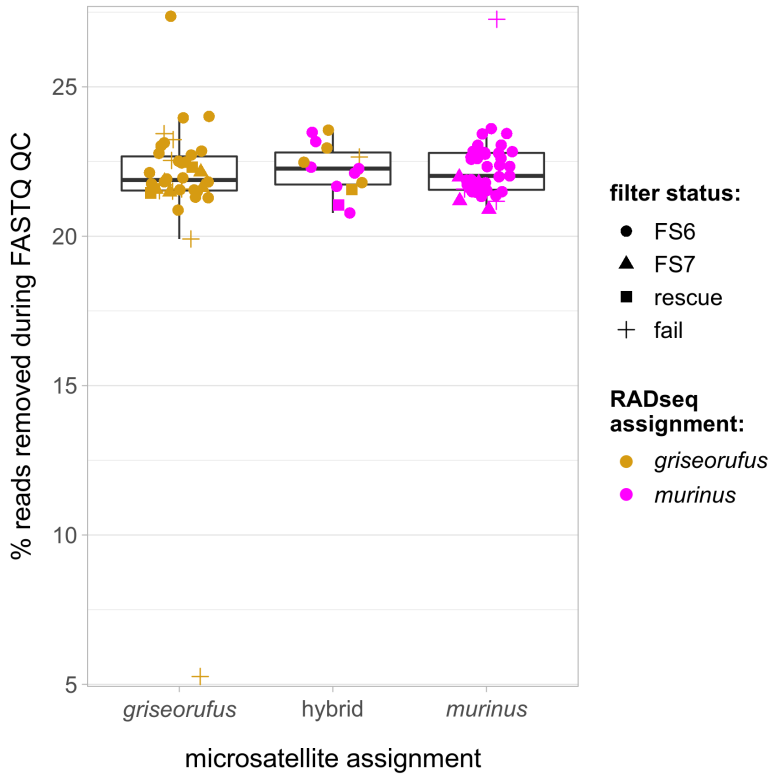

295 **Fig. S2: Percentage of reads removed by FASTQ filtering.**
Comparison across microsatellite species assignments (x-axis), RADseq species assignments (color of jittered points), and filter status (shape of jittered points).

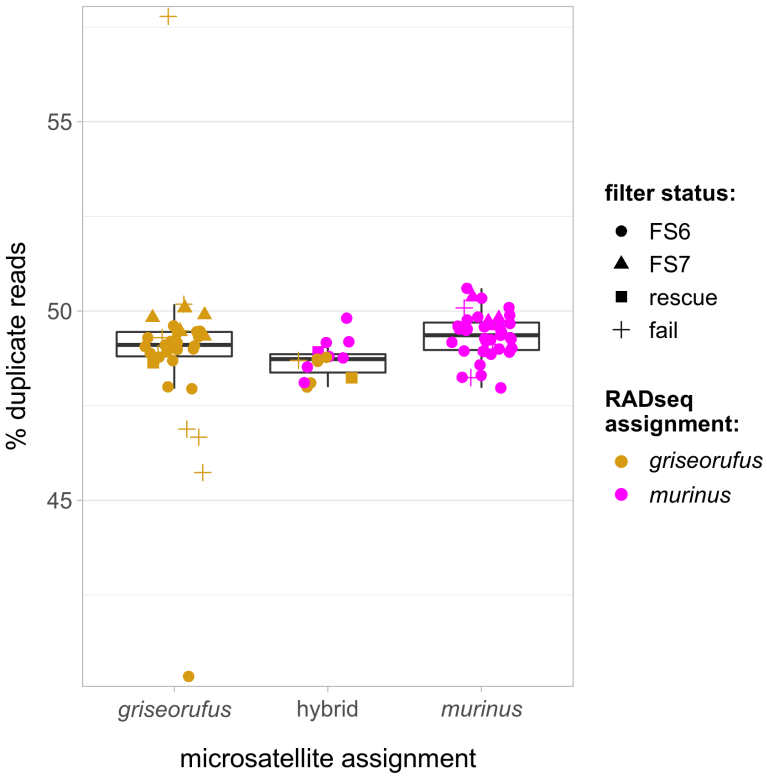

Fig. S3: Percentage of duplicate reads.
Comparison across microsatellite species assignments (x-axis), RADseq species assignments (color of jittered points), and filter status (shape of jittered points). Duplicate reads were removed prior to mapping.

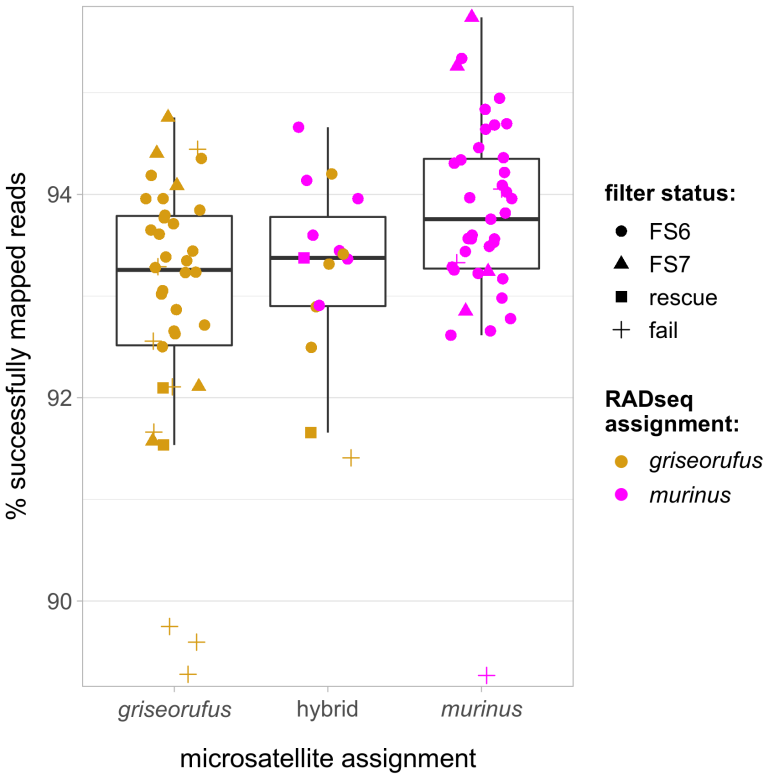

Fig. S4: Percentage of successfully mapped reads.
Comparison across microsatellite species assignments (x-axis), RADseq species assignments (color of jittered points), and filter status (shape of jittered points). Duplicate reads were removed prior to mapping.

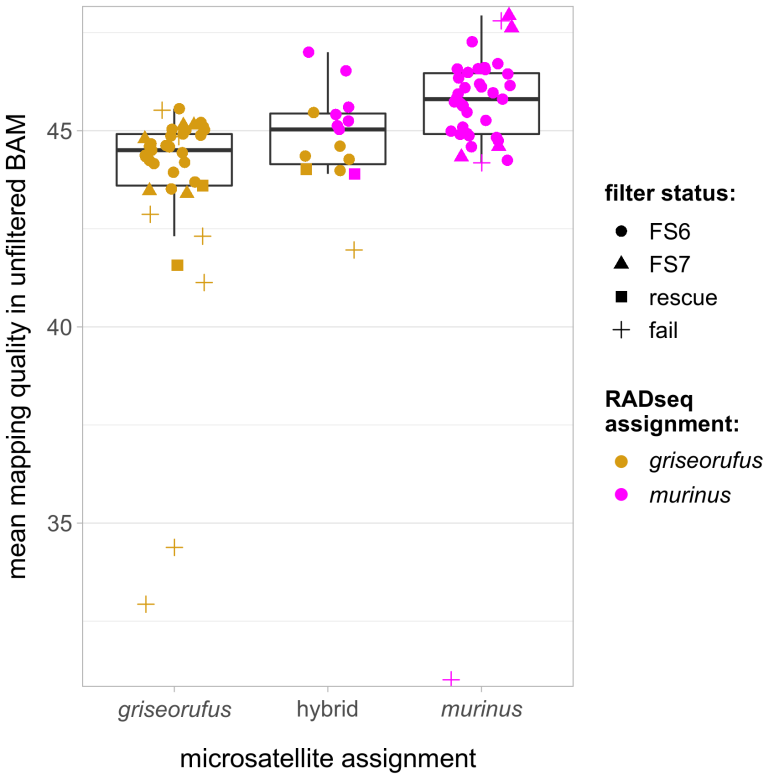

Fig. S5: Mean mapping quality in unfiltered BAM files.
Comparison across microsatellite species assignments (x-axis), RADseq species assignments (color of jittered points), and filter status (shape of jittered points).

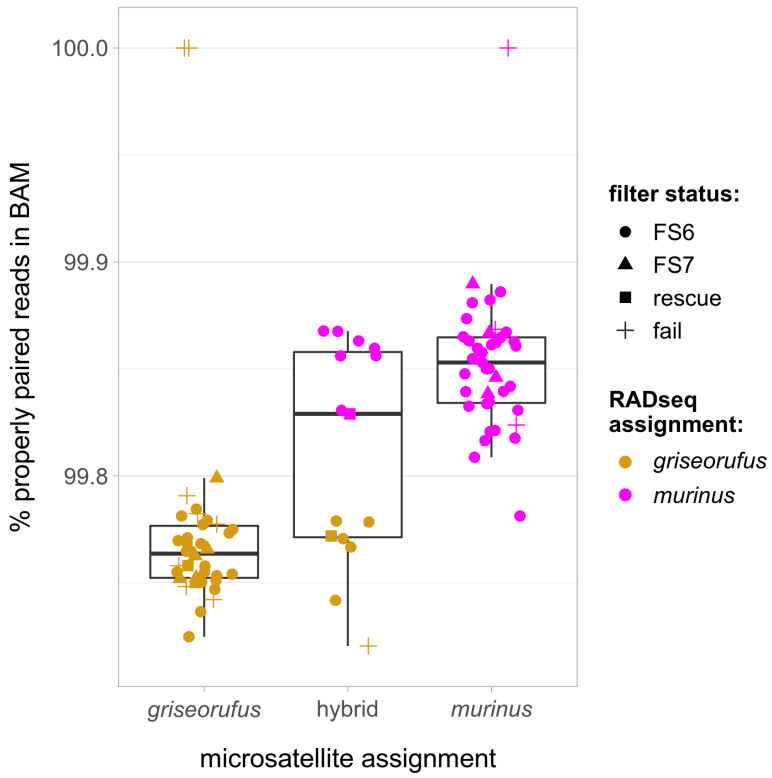

Fig. S6: Percentage of properly paired read pairs in filtered BAM files.
Comparison across microsatellite species assignments (x-axis), RADseq species assignments (color of jittered points), and filter status (shape of jittered points).

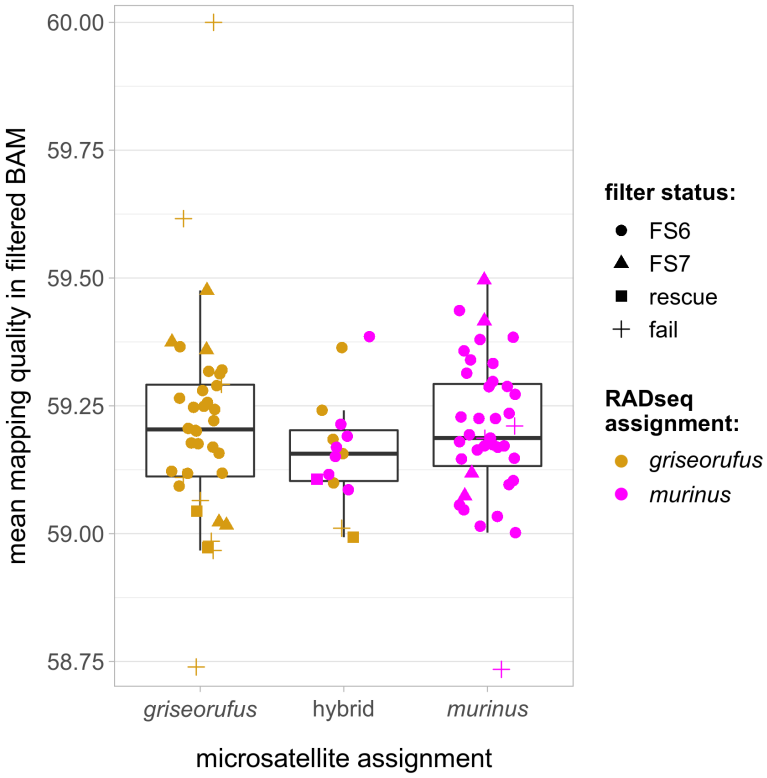

Fig. S7: Mean mapping quality in filtered BAM files.
Comparison across microsatellite species assignments (x-axis), RADseq species assignments (color of jittered points), and filter status (shape of jittered points).

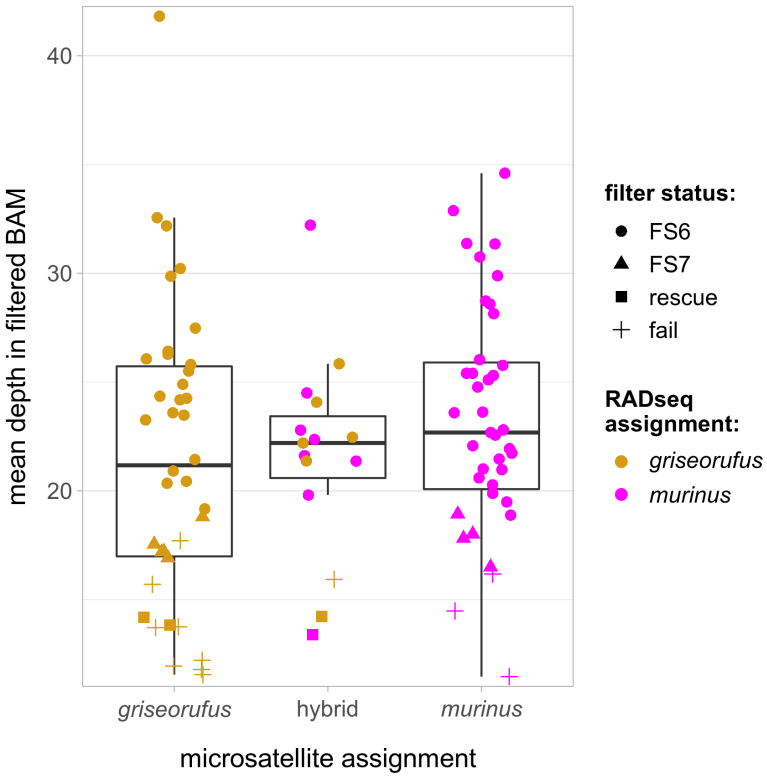

Fig. S8: Mean depth of coverage in filtered BAM files.
Comparison across microsatellite species assignments (x-axis), RADseq species assignments (color of jittered points), and filter status (shape of jittered points).

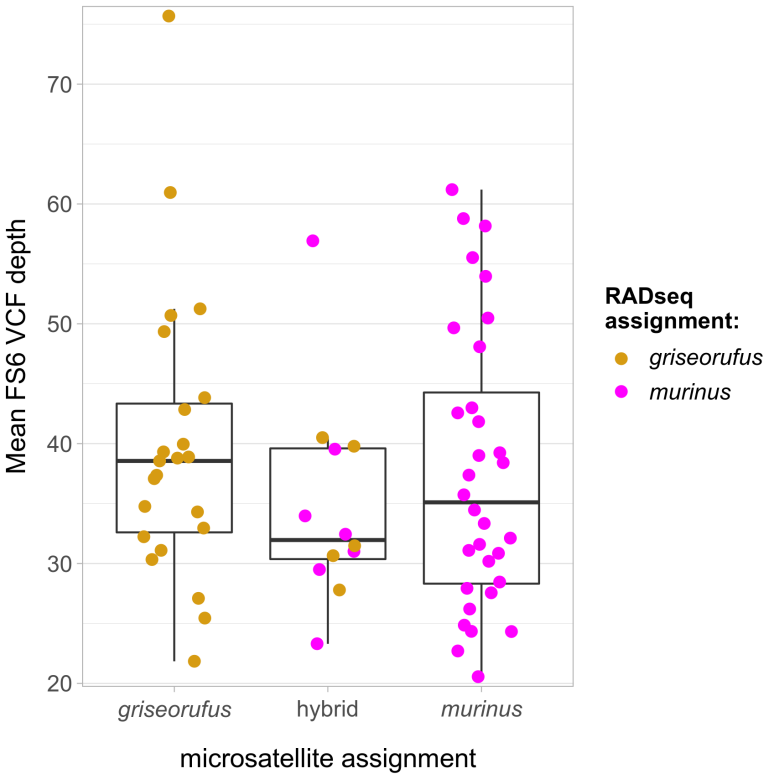

320

Fig. S9: Mean depth of coverage in the "FS6" VCF file.
Comparison across microsatellite species assignments (x-axis), RADseq species assignments (color of jittered points), and filter status (shape of jittered points). This VCF file was used for the main analyses of ancestry in the contact zone are; see Methods for details on the filtering procedure.

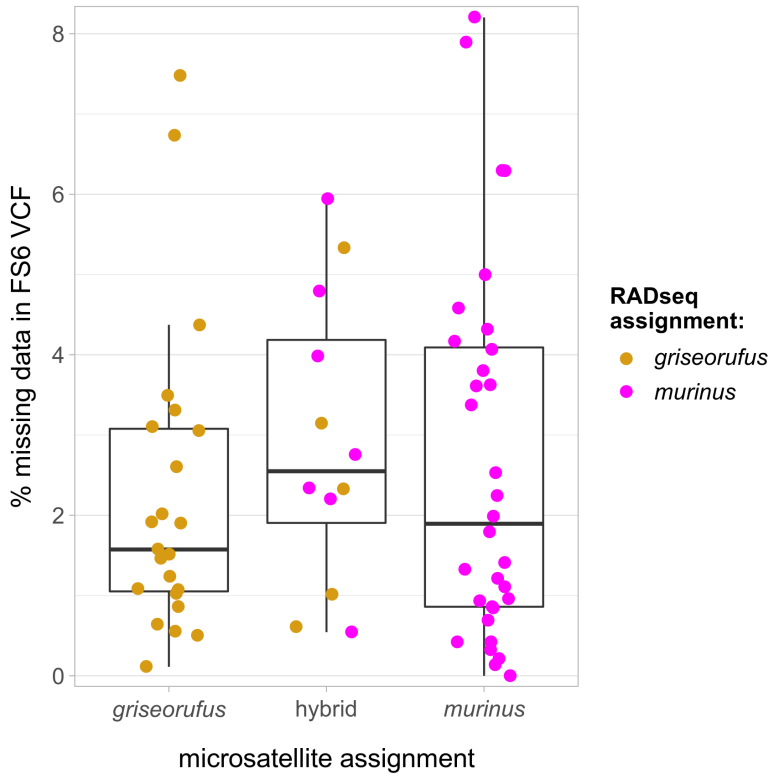

Fig. S10: Percentage of missing data in the "FS6" VCF file.
Comparison across microsatellite species assignments (x-axis), RADseq species assignments (color of jittered points), and filter status (shape of jittered points). This VCF file was used for the main analyses of ancestry in the contact zone are; see Methods for details on the filtering procedure.

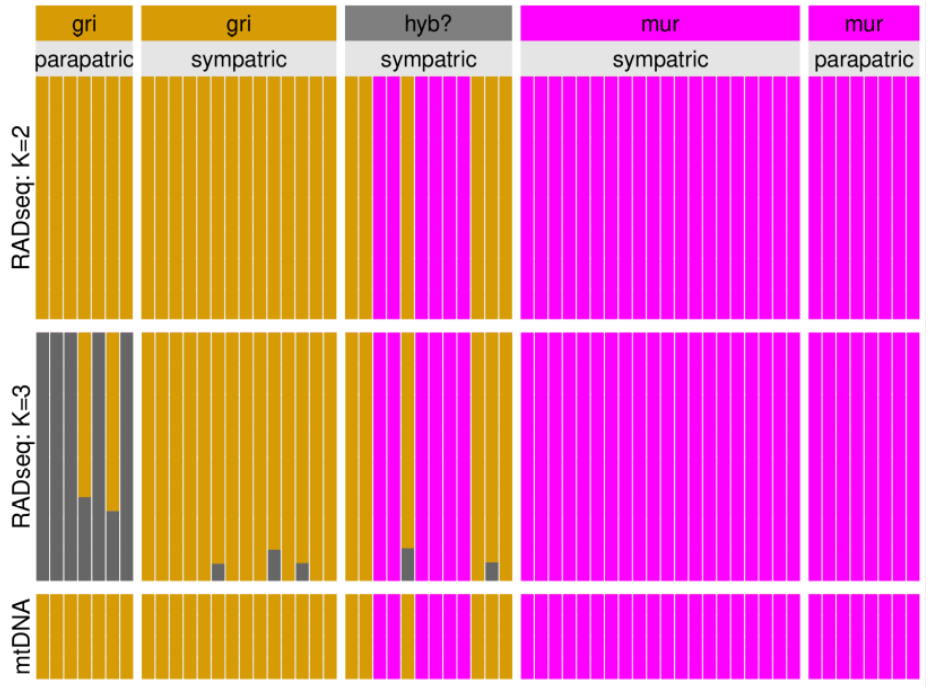

Fig. S11: ADMIXTURE results including for K=3.
The third cluster relates to differentiation in *griseorufus*, between parapatric (Hazofotsy) and sympatric (Mangatsiaka, Tsimelahy) sites.

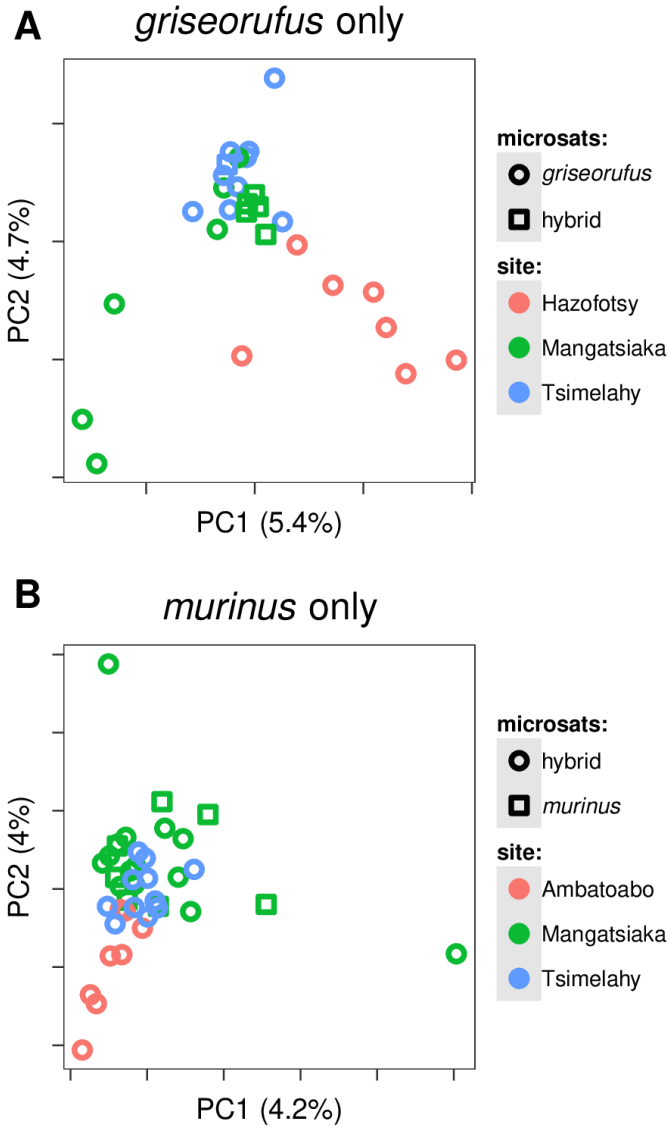

335

Fig. S12: Within-species PCAs
The “microsats” designation indicates how Hapke et al. (2011) classified the sample using microsatellites.

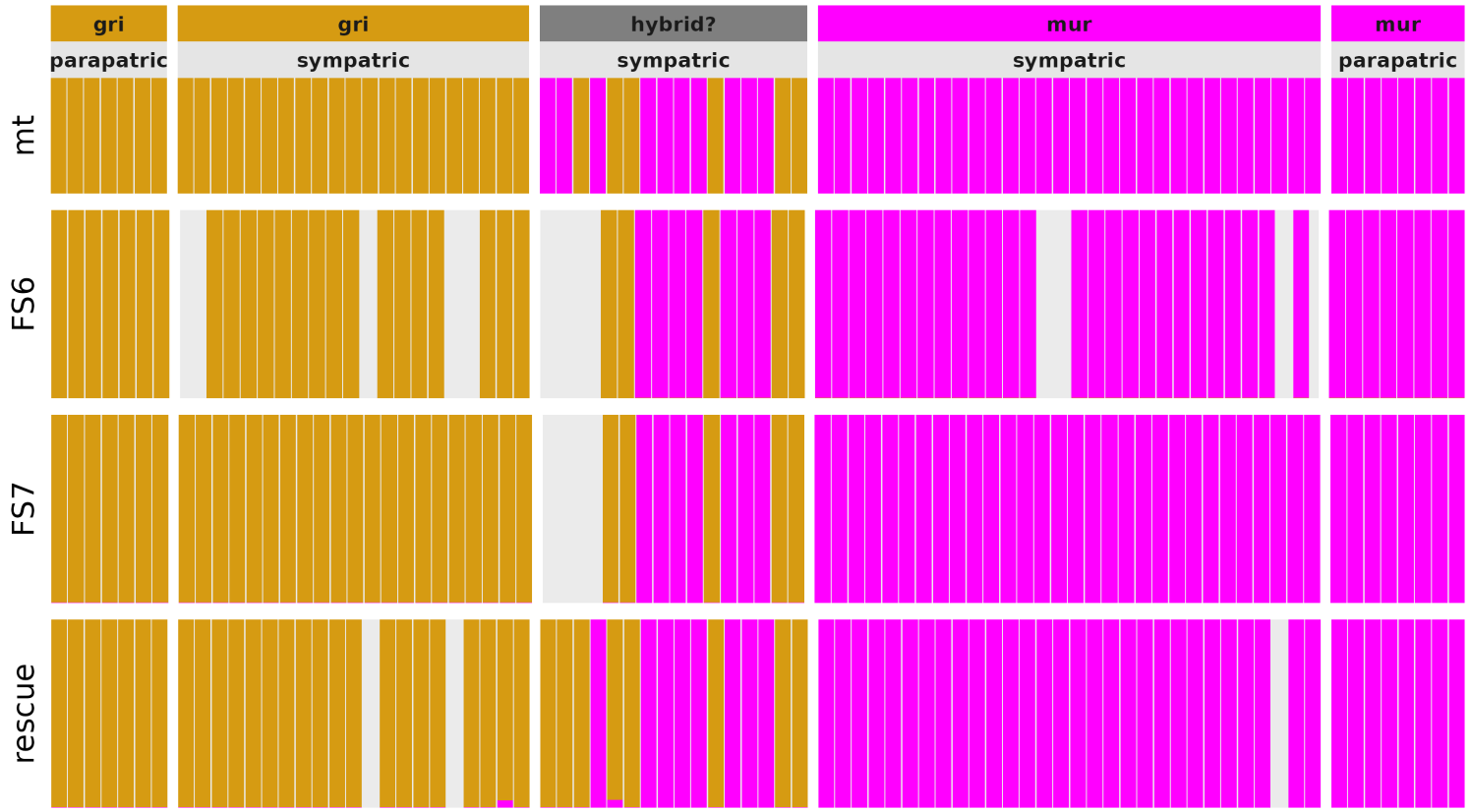

Fig. S13: ADMIXTURE results for different filtering options
Gray areas indicate that the samples in question were not present in the focal VCF file. Two samples (mhyb001 and mhyb002) only present in the "rescue" dataset show *griseorufus* nuclear DNA, but a *murinus* mitochondrial haplotype, in line with results from Lüdemann (2018). Two other samples (mhyb003 and mgri104) show <5% *murinus* ancestry in the "rescue" dataset, but these samples did not show any *murinus* ancestry in the FS6 and FS7 datasets, which contain many more SNPs and are therefore more reliable.

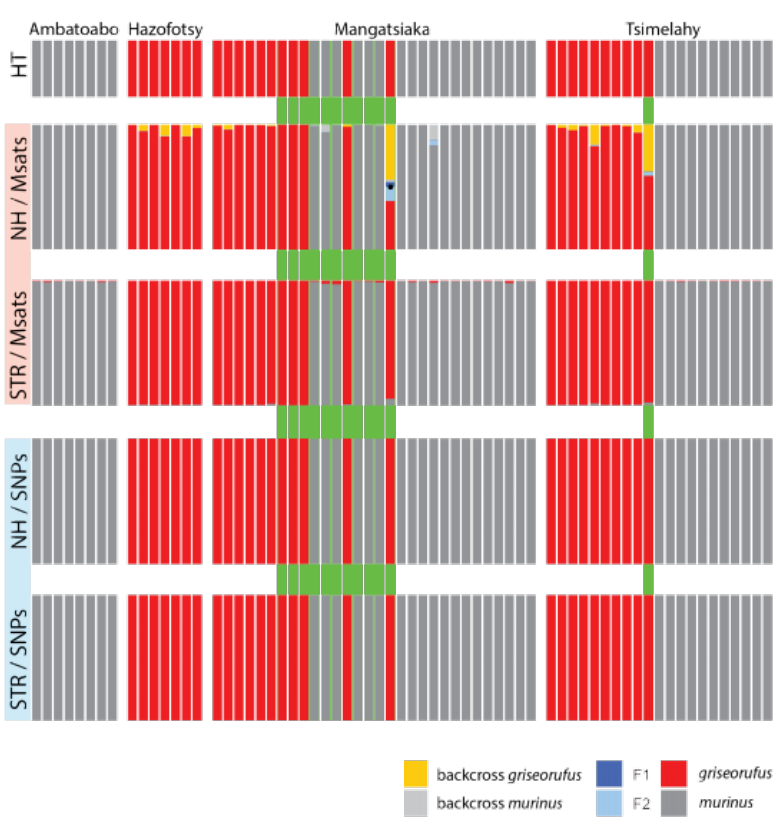

Fig. S14: Re-analysis of microsatellite data for individuals with RADseq data.
Top row: mitochondrial haplotype (HT).
Next two rows: microsatellites (Msats) analysed with NewHybrids (NH) and Structure (STR).
Bottom two rows: RADseq SNPs (SNPs) analysed with NewHybrids (NH) and Structure (STR).

While no hybrids are detected using RADseq data, NewHybrids identifies a single hybrid (black dot) using the microsatellite data, with several further *griseorufus* individuals showing non-significant signs of admixed ancestry (yellow ancestry).

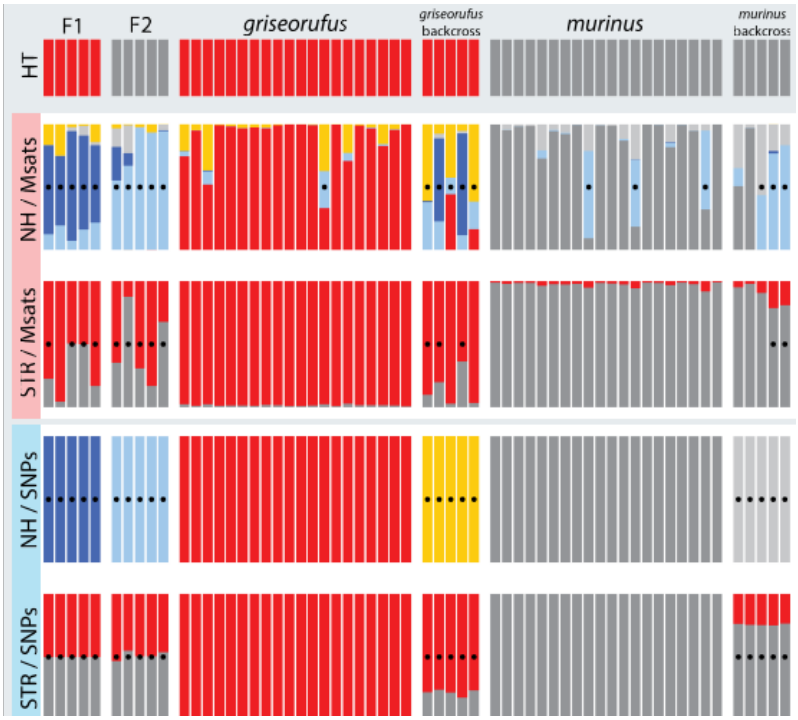

Fig. S15: Assignment of simulated individuals using microsatellites and SNPs with Structure and Newhybrids.
A black dot indicates that a given sample was classified as a hybris.
HT: mitochondrial haplotype, NH: NewHybrids, STR: Structure, SNPs: RADseq SNP, Msats: microsatellites.

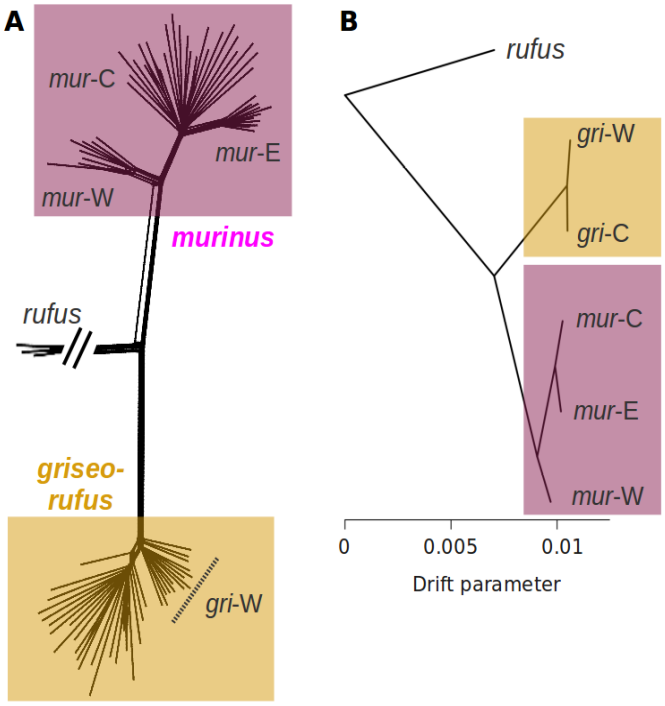

Fig. S15: Phylogenetic relationships.
A) A `SplitsTree` NeighborNet phylogenetic network. Each tip represents an individual, and the width of any edge boxes depicts phylogenetic conflict, which can be due to incomplete lineage sorting or admixture. Very little conflict is observed along the edges between *griseorufus* and *murinus*. *Murinus* is separated into three clades which correspond to western (*mur*-W), contact zone area (*mur*-C), and eastern (*mur*-E) populations. The separation of *griseorufus* into clades corresponding to western (*gri*-W) and contact zone area (*gri*-C) populations is not as well-defined.
B) Treemix results with no migration edges. Treemix supports the relationships suggested by the phylogenetic network, with western *murinus* (*mur*-W) being the most divergent among the three *murinus* populations.

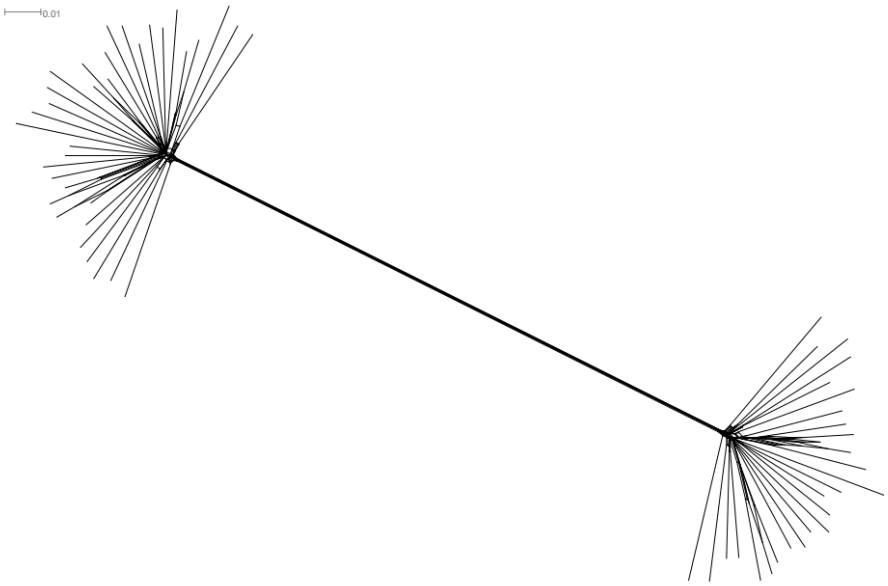

Fig. S16: A SplitsTree NeighborNet phylogenetic network using only contact zone individuals.

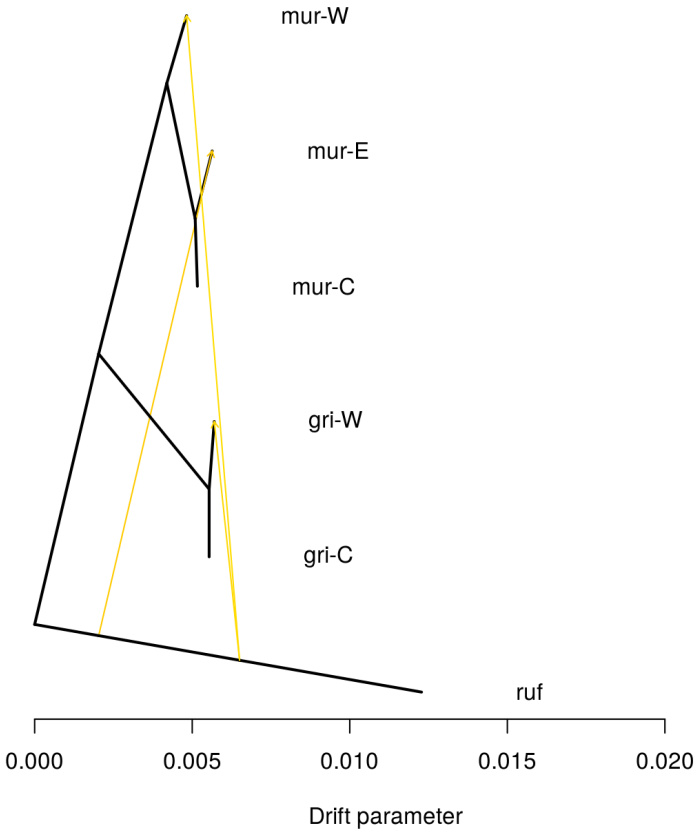

375

Fig. S17: Significant migration edges using Treemix (with *M. rufus)*.
All three migration edges are minor and involve *M. rufus*.

380

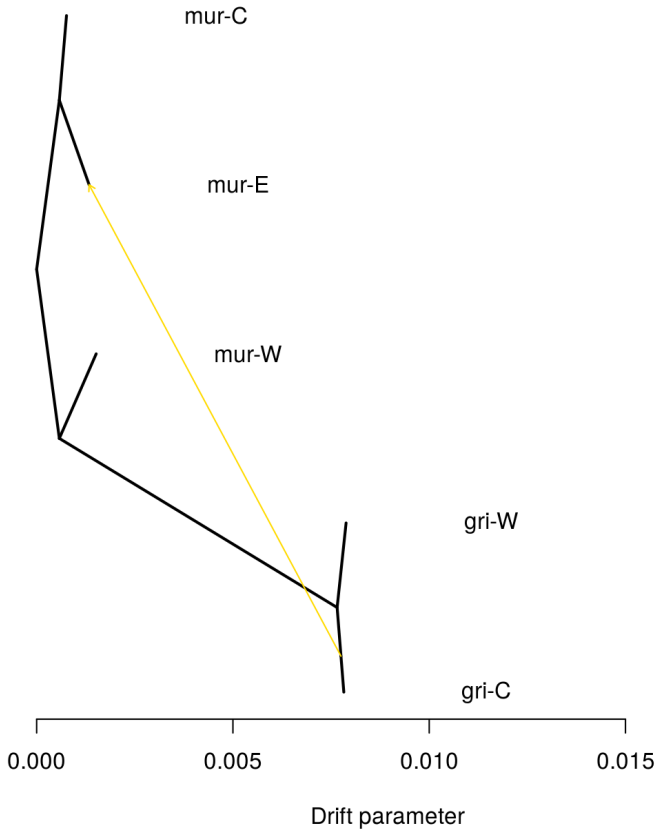

Fig. S18: Significant migration edges using Treemix (without *M. rufus)*.

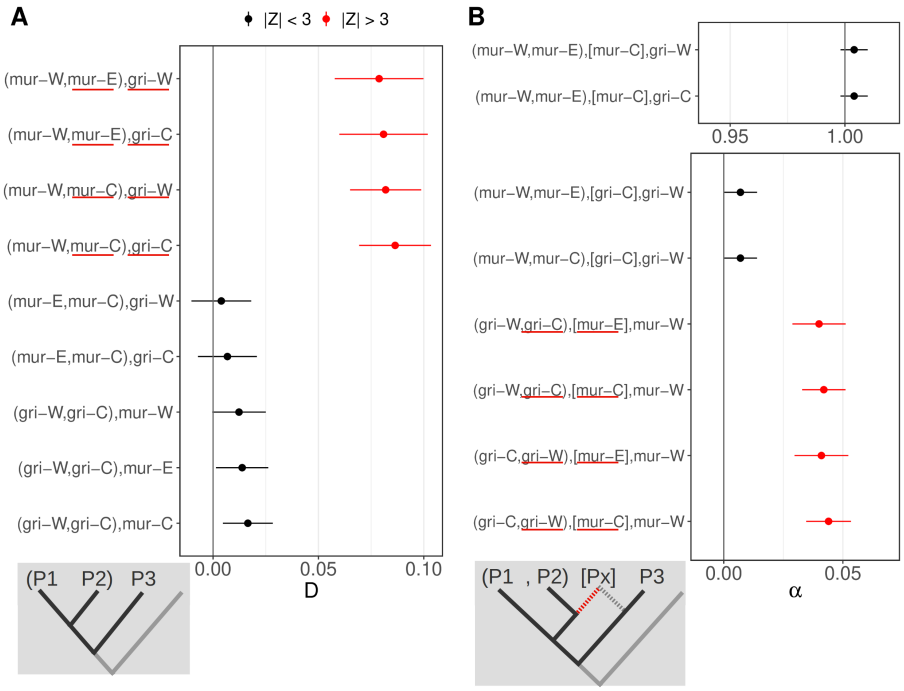

Fig. S20: Admixture statistics suggest some ancestral but no contemporary gene flow.
A) D-statistics. Focal comparisons are listed as `(P1,P2),P3` and test for admixture between P3 and P1 (negative D) or P2 (positive D). Populations inferred to have experiences admixture are underlined in red. For all tests, *M. rufus* was used as the outgroup (O/P4). In the top 4 rows, with *mur*-W as P1, D is significant and highly similar regardless of which *griseorufus* population (*gri*-W or *gri*-C) is used as P3 and regardless of which southeastern *murinus* population (*mur*-E or *mur*-C) is used as P2. This suggests historical but no ongoing admixture between the ancestral *griseorufus* and southeastern *murinus* lineages. A lack of ongoing gene flow is also supported by non-significant results for the bottom five comparisons.
B) f_4-ratio tests. Focal comparisons are listed as `(P1,P2),[Px],P3)`, where Px is tested for being a mixture between P2 and P3. On the x-axis, α indicates the proportion of P2 ancestry in Px (α=1 if Px is sister to P2 with no admixture from P3, and α=0 if Px is sister to P3 with no admixture from P2). Admixture is inferred if α is significantly different from 0 and 1 (red dots). Consistent with results for D-statistics, admixture is inferred between the two southeastern *murinus* populations and both *griseorufus* populations, with values of α highly similar regardless of which *griseorufus* population (*gri*-W or *gri*-C) is used as P1 and which as P2, and regardless of which southeastern *murinus* population (*mur*-E or *mur*-C) is used as Px.

5 References

Bolger A.M., Lohse M., Usadel B. 2014. Trimmomatic: a flexible trimmer for Illumina sequence data. Bioinformatics. 30:2114–2120.

Earl D.A., vonHoldt B.M. 2012. STRUCTURE HARVESTER: a website and program for visualizing STRUCTURE output and implementing the Evanno method. Conservation Genet Resour. 4:359–361.

Evanno G., Regnaut S., Goudet J. 2005. Detecting the number of clusters of individuals using the software structure: a simulation study. Molecular Ecology. 14:2611–2620.

Gilbert K.J., Andrew R.L., Bock D.G., Franklin M.T., Kane N.C., Moore J.-S., Moyers B.T., Renaut S., Rennison D.J., Veen T., Vines T.H. 2012. Recommendations for utilizing and reporting population genetic analyses: the reproducibility of genetic clustering using the program structure. Molecular Ecology. 21:4925–4930.

Hapke A., Gligor M., Rakotondranary S.J., Rosenkranz D., Zupke O. 2011. Hybridization of mouse lemurs: different patterns under different ecological conditions. BMC Evolutionary Biology. 11:297.

Li H. 2013. Aligning sequence reads, clone sequences and assembly contigs with BWA-MEM. arXiv:1303.3997 [q-bio].

Li H., Handsaker B., Wysoker A., Fennell T., Ruan J., Homer N., Marth G., Abecasis G., Durbin R., 1000 Genome Project Data Processing Subgroup. 2009. The Sequence Alignment/Map format and SAMtools. Bioinformatics. 25:2078–2079.

Lüdemann J. 2018. Re-assessment of a lemur hybrid zone using mitochondrial and nuclear data. BSc thesis, Universität Hamburg.

O'Leary S.J., Puritz J.B., Willis S.C., Hollenbeck C.M., Portnoy D.S. 2018. These aren't the loci you're looking for: Principles of effective SNP filtering for molecular ecologists. Mol. Ecol. 27:3193–3206.

Pritchard J.K., Stephens M., Donnelly P. 2000. Inference of population structure using multilocus genotype data. Genetics. 155:945–959.

Rochette N.C., Rivera-Colón A.G., Catchen J.M. 2019. Stacks 2: Analytical methods for paired-end sequencing improve RADseq-based population genomics. Molecular Ecology. 28:4737–4754.